Tellus (1995), 47B, 447–460
Printed in Belgium – all rights reserved

TELLUS
ISSN 0280–6509

Air-sea exchange of CO_2 in the central and western equatorial Pacific in 1990

By MASAO ISHII* and HISAYUKI YOSHIKAWA INOUE, *Geochemical Research Department, Meteorological Research Institute, Nagamine 1-1, Tsukuba, Ibaraki, 305 Japan*

(Manuscript received 27 December 1993; in final form 21 February 1995)

ABSTRACT

Measurements of CO_2 in marine boundary air and in surface seawater of the central and western Pacific west of 150°W were made during the period from September to December 1990. The meridional section along 150°W showed pCO_2(sea) maximum over 410 μatm between the equator and 3°S due to strong equatorial upwelling. In the equatorial Pacific between 150°W and 179°E, pCO_2(sea) decreased gradually toward the west as a result of biological CO_2 uptake and surface sea temperature increase. Between 179°E and 170°E, the pCO_2(sea) decreased steeply from 400 μatm to 350 μatm along with a decrease of salinity. West of 170°E, where the salinity is low owing to the heavy rainfall, pCO_2(sea) was nearly equal to pCO_2(air). The distribution of the atmospheric CO_2 concentration showed a considerable variability (± 3 ppm) in the area north of the Intertropical Convergence Zone due to the regional net source-sink strength of the terrestrial biosphere. The net CO_2 flux from the sea to the atmosphere in the equatorial region of the central and western Pacific (15°S–10°N, 140°E–150°W) was evaluated from the ΔpCO_2 distribution and the several gas transfer coefficients reported so far. It ranged from 0.13 GtC year^{-1} to 0.29 GtC year^{-1}. This CO_2 outflux is thought to almost disappear during the period of an El Niño event.

1. Introduction

The intrusion of bomb-produced ^{14}C into the ocean soon after the intensive atmospheric nuclear tests in the early 1960s revealed an extensive CO_2 exchange between the air and the sea (Nydal and Lövseth, 1983; Broecker et al., 1985). The gross fluxes of the atmospheric CO_2 into the ocean have been assessed to be 74 GtC year^{-1} in the pre-industrial era and 92 GtC year^{-1} during the 1980s, which corresponds to 12% of the total atmospheric CO_2 content (Siegenthaler, 1986; IPCC, 1990; Siegenthaler and Sarmiento, 1993). However, the global net CO_2 flux between the sea and the air is still not fully documented. The accumulation of regional net air-sea CO_2 flux ($F(CO_2)$) data over the world ocean is one of the reasonable approaches to evaluate the global net CO_2 flux. The regional net CO_2 flux is still useful in constraining the atmospheric CO_2 transport models for assessing the global CO_2 budget. It can be estimated using equation (1):

$$F(CO_2) = E(pCO_2(\text{sea}) - pCO_2(\text{air})) = E\,\Delta pCO_2 \quad (1)$$

where E is the gas transfer coefficient of CO_2 between the sea and the air, pCO_2(sea) the partial pressure of CO_2 in surface seawater, and pCO_2(air) the partial pressure of CO_2 in the surface air equilibrated with water vapor.

pCO_2(sea) shows greater spatial and temporal variabilities than pCO_2(air). For example, pCO_2(sea) in the subtropical region of the western North Pacific ranges from 300 μatm in winter to about 400 μatm in summer (Fushimi, 1987; Inoue et al. 1987; Inoue and Sugimura, 1988a; JMA, 1991, 1992). Several authors have reported high pCO_2(sea) close to 450 μatm in the equatorial

* Corresponding author.

Pacific (Feely et al., 1987; Murphy et al., 1991a, 1991b; Inoue and Sugimura, 1992; Lefevre and Dandonneau, 1992; Wong et al., 1993). However, there are not enough direct shipboard measurements of pCO_2(sea) to describe its large spatial and temporal variations. Therefore, it is necessary to distinguish the factors that dominate pCO_2(sea) variations and deduce pCO_2(sea) from other parameters for which more frequent observations are available, in order to properly interpolate between and extrapolate from the existing data.

There are several factors that alter the pCO_2(sea): (a) Change in sea surface temperature (SST) due to heat flux and change in salinity due to fresh water flux, which alter the solubility of CO_2 in sea water (Weiss, 1974) and dissociation constants of carbonic acid and bicarbonate (Dickson and Millero, 1987) (thermodynamic effect) (b) Net CO_2 absorption or emission due to CO_2 exchange through the air-sea interface. The large Revelle factor (≈ 10) (Wagner, 1979) indicates that significant changes in pCO_2(sea) will occur only with small changes in the total dissolved inorganic carbon (DIC) content of seawater. They result from shifts in chemical equilibria (and consequent pH changes) as CO_2 is removed from or added to surface waters. (c) Biological activity such as CO_2 fixation by photosynthesis and CO_2 discharge by respiration or decomposition of organic matter. They also change the DIC content and pH like air-sea CO_2 net exchange. (d) The activity of calcareous algae which deposit massive calcium carbonate during photosynthesis (Okazaki, 1993) and dissolution of calcium carbonate. The deposition of calcium carbonate reduces the alkalinity and pH, hence it elevates pCO_2(sea). As a result of differences in the contribution of these factors, different water masses have different pCO_2(sea) and the vertical variation of pCO_2(sea) occurs. Therefore, lateral and vertical mixing, and upwelling can also cause spatial and temporal pCO_2(sea) variations.

The upper layer of the ocean in the equatorial Pacific is characterized by complicated vertical and horizontal circulations (Philander, 1990) and higher primary production (Berger, 1989). It is also the largest CO_2 source region of the ocean, where the distribution of pCO_2(sea), and hence the net air-sea CO_2 flux, is known to exhibit a large variability associated with El Niño-Southern Oscillation (ENSO) event to the extent that they may affect the growth rate of the atmospheric CO_2 concentration (Keeling and Revelle, 1985; Feely et al., 1987; Fushimi, 1987; Inoue and Sugimura, 1988b; Inoue and Sugimura, 1992; Wong et al., 1993). We report here the pCO_2(sea) and atmospheric CO_2 concentration in and over the equatorial Pacific west of 150° W observed in 1990, and discuss the factors that influence the pCO_2(sea) distribution in this region. We also attempt to estimate the net CO_2 flux between the sea and the air on the basis of the ΔpCO_2 using the various gas exchange coefficients given by different authors.

2. Observations

2.1. Cruise track

We made continual observations of CO_2 concentration in the marine boundary air (CO_2(air)) and in the air equilibrated with surface seawater (CO_2(sea)) in the central and western Pacific west of 150° W from September through December 1990. The observations were made during the KH-90-2 and KH-90-3 cruises of the R.V. Hakuhomaru belonging to the Ocean Research Institute, the University of Tokyo. The cruise track is shown in Fig. 1. Monthly SST anomalies were +0.6°C or +0.7°C in the central equatorial Pacific (from 160° E to 150° W between 4° N and 4° S), +0.1°C or +0.2°C in the eastern Pacific (from 150° W to 90° W between 4° N and 4° S), and the Southern Oscillation Index was between 0.0 and −0.8

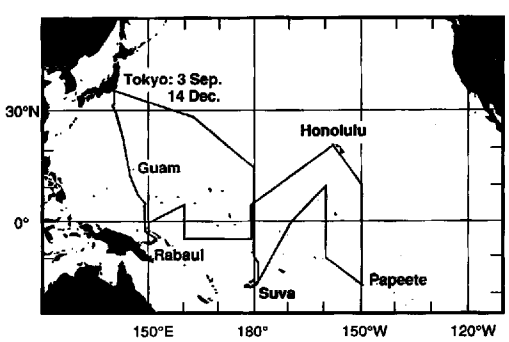

Fig. 1. Cruise tracks of KH-90-2 and KH-90-3 of the R. V. Hakuho-maru. KH-90-2 is from Tokyo (September 3, 1990) to Honolulu (Hawaii) (October 25, 1990) via Suva (Fiji) and Papeete (Tahiti). KH-90-3 is from Honolulu (October 31, 1990) to Tokyo (December 14, 1990) via Rabaul (Papua New Guinea) and Guam.

(JMA, 1993a). These modest values suggest that it had been under a non-El Niño condition during the time of observations.

2.2. *Measurements*

We used an automatic CO_2 analyzer for the CO_2 measurements. For the CO_2(air) measurement, a sample of air (0.6–0.7 dm^3 min^{-1}) pumped continuously from the bow of the ship was dried and introduced into the non-dispersive infrared gas analyzer (NDIR analyzer; Model 865, Beckman). For the CO_2(sea) measurement, seawater pumped up continuously from the bottom of the ship was introduced into a shower-type equilibrator, where it was equilibrated with the air in a closed circuit. The seawater-equilibrated air was dried and introduced into the NDIR analyzer. All NDIR output voltages were recorded under the ambient pressure while stopping the air stream temporarily, and they were calibrated once an hour using four CO_2-in-air working standard gases (279 ppm, 340 ppm, 361 ppm, 421 ppm). These gases were calibrated before and after the cruise against the standard gases (Nippon Sanso Co., Japan) prepared by a gravimetric method in the same way as reported by Tanaka et al. (1987). The details of the system and procedure are basically the same as described by Inoue et al. (1987) and Inoue and Sugimura (1992).

Values of pCO_2(sea) were corrected for seawater warming in the inner piping of the ship (mostly below +0.4°C) using the relationship given by Gordon and Jones (1973);

$$dpCO_2(\text{sea})/dT = 4.4 \times 10^{-2}(pCO_2(\text{sea})) - 4.6 \times 10^{-6}(pCO_2(\text{sea}))^2. \quad (2)$$

DIC content of seawater was determined by a coulometric DIC measurement apparatus after the cruise for some preserved surface seawater samples. They were collected in 120 cm^3 gas-tight bottles at some hydrographic stations and 0.2 cm^3 saturated mercury(II) chloride solution was added to inhibit biological activities.

Air samples for the measurement of $\delta^{13}C$ of the CO_2 were collected in 5 dm^3 glass flasks (Pyrex glass, 130 mm dia) with Teflon O-ring stop-cocks at both ends. After purifying the CO_2, $\delta^{13}C$ was measured with the mass spectrometer (MAT 250, Finnigan) as described previously by Inoue and Sugimura (1992). N_2O corrections have not been made in this report.

The ship position, SST, atmospheric pressure, wind direction and wind speed were recorded once every 5 min during both cruises. Several oceanic properties were observed at several stations using a CTD/rosette-multi-sampler. Ocean current observations in the upper layer by the Acoustic Doppler Current Profiler were made in the same cruise.

2.3. *Data selection of the CO_2 data*

Apart from the natural variability, atmospheric CO_2 data fluctuates due mainly to contamination of air from the ship and the instability of the NDIR analyzer in rough sea conditions. Obvious contaminated data, as revealed when the ship is in stoppage at stations, were excluded from the data set. The data falling outside of 1.5 standard deviation (1.5σ) from the average of the data at each degree of latitude were also rejected. Through this procedure, 6.4% of the atmospheric CO_2 data were omitted from the data set.

As CO_2 in surface seawater exhibits a greater variability, data selection of CO_2 must be done with care. Suspicious data due to the stoppage or shortage of seawater supply, leakage of air from the closed circuit of the system, etc. were excluded first. Then the data exceeding 3σ from the average of the data of each degree of latitude were rejected. Through this procedure, 0.4% of the oceanic CO_2 data were omitted from the data set.

3. Results and discussion

3.1. *Distribution of the atmospheric CO_2 concentration*

Meridional distributions of CO_2 concentration in marine boundary air in September and December along the ship track are shown in Fig. 2a and Fig. 2b, respectively. Corresponding CO_2 data from land stations (WMO, 1992), superposed on the plot, are in excellent agreement with our shipboard observation data. In September, a steep gradient of CO_2 concentration appeared around 9°N. This zone can be identified as the Intertropical Convergence Zone (ITCZ) on the basis of the high-cloud distribution data in this season (JMA, 1990a, 1990b, 1990c, 1990d). Methane concentration had also exhibited a steep

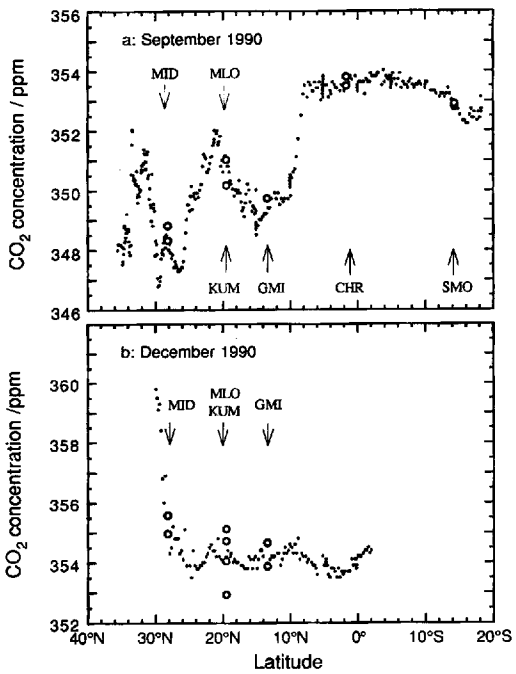

Fig. 2. Meridional distribution of CO_2 concentration in the marine boundary air. (a) in September, 1990. (b) in December, 1990. Data from land stations are shown by open circles with their respective NOAA codes.

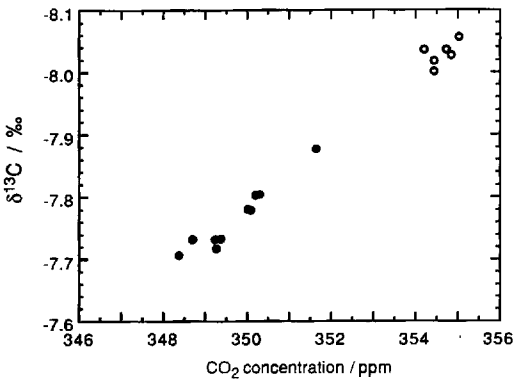

Fig. 3. Relationship between atmospheric CO_2 concentration and $\delta^{13}C$ north of the Intertropical Convergence Zone. Closed circles: in September 1990. Open circles: in December 1990.

gradient at the same location in the same cruise, which is thought to be the result of the strong source of methane in the Northern Hemisphere and the restricted north-south air mixing at the ITCZ (Matsueda et al., 1993). The steep gradient of the CO_2 concentration at the ITCZ is attributable to the strong sink of the terrestrial biosphere in the Northern Hemisphere in boreal summer and the restricted north-south air mixing.

Concentration of CO_2 in September kept an almost uniform distribution ranging from 353 ppm to 354 ppm between the ITCZ and 10°S with an indistinct maximum around 4°S. North of the ITCZ, CO_2 concentration exhibited a large variability ranging from 347 ppm to 352 ppm with 4 distinct peaks between 10°N and 35°N. The reason for this large variability is not clear at the moment, but the linear relationship between CO_2 concentration and the $\delta^{13}C$ of CO_2 ($-0.05‰$ ppm^{-1}) for the area north of the ITCZ in September, shown in Fig. 3, suggests that it is related to the difference in the regional CO_2 source-sink strength of the terrestrial biosphere (Keeling, 1958, 1961).

In December, the atmospheric CO_2 concentration showed an almost uniform meridional distribution between the equator and 25°N as a result of the seasonal strengthening of the net CO_2 emission from the terrestrial biosphere in the Northern Hemisphere and the seasonal abatement of the ITCZ especially in the western Pacific (JMA, 1990d). The higher CO_2 concentration in the north of 25°N off Japan will be the influence of the air with biospheric and/or fossil fuel origin from land (Inoue et al., 1987).

3.2. Meridional distributions of pCO_2 in surface seawater

Figs. 4a–4e show the meridional distributions of pCO_2(air), pCO_2(sea), and SST along 150°W, 160°W, 180°, 179°E, and 160°E, respectively. In the equatorial zone, the pCO_2(sea) showed supersaturation with its maximum between 0° and 6°S, while it was equal to or even lower than pCO_2(air) south of 15°S. On the North Equatorial Counter Current (NECC) flowing eastward between 5°N and 10°N and conveying less saline water (below 34 psu), the pCO_2(sea) was almost the same level as pCO_2(air) for all meridional sections.

In the meridional section along 150°W, pCO_2(sea) maximum exceeded 440 μatm between 0° and 2°S, and it coincided with the SST minimum, nitrate maximum, and chlorophyll maximum which indicate the influence of maximum upwell-

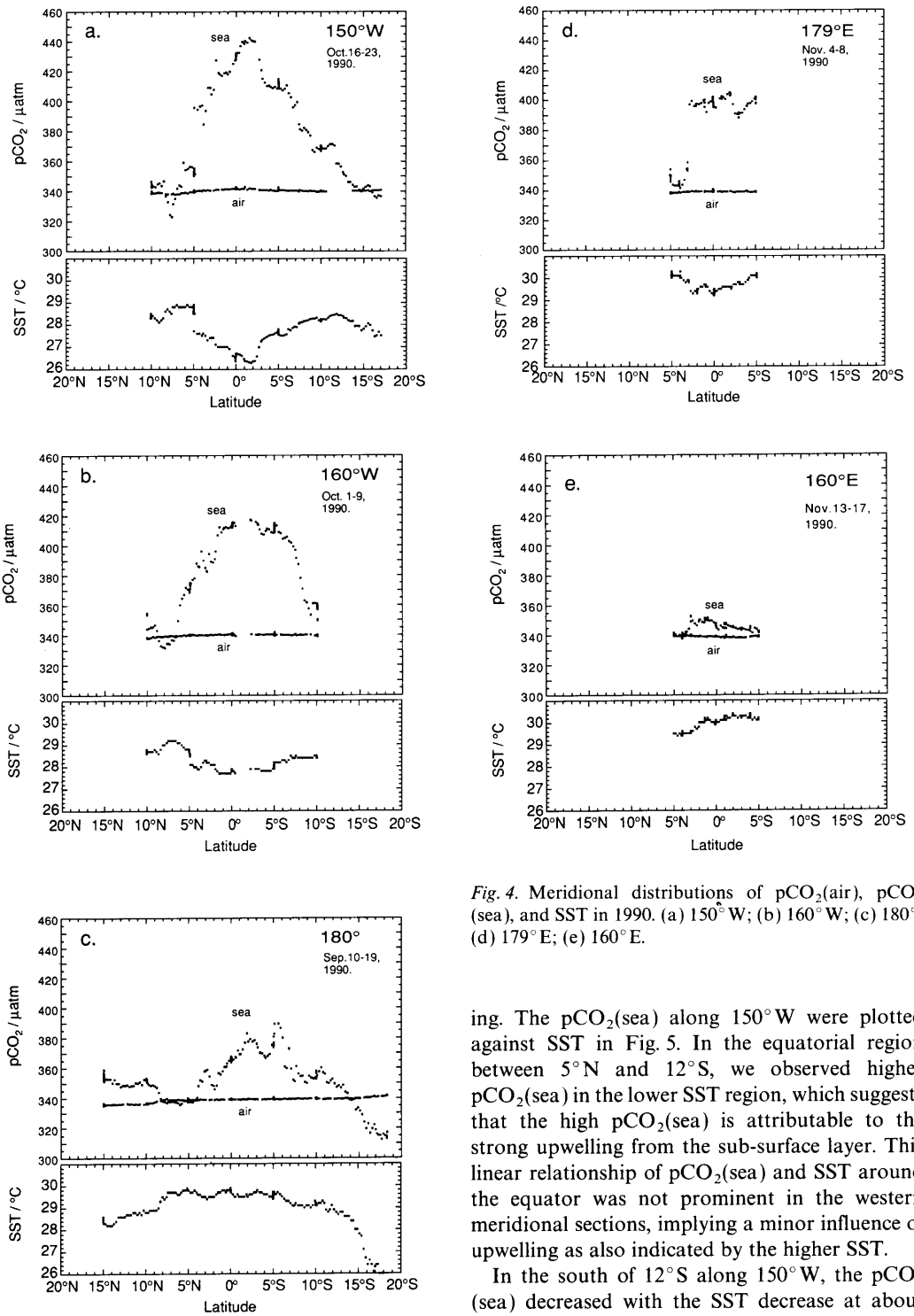

Fig. 4. Meridional distributions of pCO_2(air), pCO_2 (sea), and SST in 1990. (a) 150° W; (b) 160° W; (c) 180°; (d) 179° E; (e) 160° E.

ing. The pCO_2(sea) along 150° W were plotted against SST in Fig. 5. In the equatorial region between 5° N and 12° S, we observed higher pCO_2(sea) in the lower SST region, which suggests that the high pCO_2(sea) is attributable to the strong upwelling from the sub-surface layer. This linear relationship of pCO_2(sea) and SST around the equator was not prominent in the western meridional sections, implying a minor influence of upwelling as also indicated by the higher SST.

In the south of 12° S along 150° W, the pCO_2 (sea) decreased with the SST decrease at about

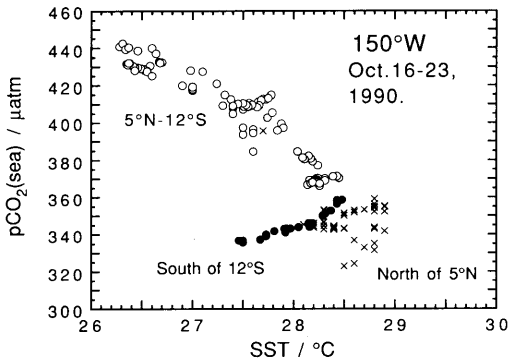

Fig. 5. Relationship between pCO_2(sea) and SST at 150°W.

4.5% $°C^{-1}$ (Fig. 5). It is close to the rate expected from the proposed relationships between pCO_2 (sea) and SST at constant DIC, alkalinity, and salinity such as that given by Gordon and Jones (1973) and that given by Weiss et al. (1982). This is also the case in the south of 10°S along 180°. Therefore, meridional distributions of pCO_2(sea) as well as seasonal variation of pCO_2(sea) (Weiss, et al., 1982) are principally attributable to the thermodynamic effects in these parts of the subtropical gyre in the South Pacific.

The pCO_2(sea), salinity, and DIN (nitrate and nitrite) concentration between 5°N and 5°S along 180° observed from 13–17 September are lower than those along 179°E observed from 4–8 November (Table 1). According to the Levitus seasonal climatology for salinity (Levitus, 1982), the averaged salinity from 5°S to 5°N at 180° is larger than 35 over the period August to January. Therefore, the seawater with its mean salinity 34.778 between 5°S and 5°N along 180° in September 1990 is thought to had been a bit affected by temporary larger freshwater influx due to prior heavy rainfall.

The pCO_2(sea) along 160°W, 180°, and 160°E had been observed in January–February 1987 during the 1986/87 El Niño and in January–February 1989 during the 1988/89 La Niña. The pCO_2(sea) during the 1988/89 La Niña was much higher than that during the El Niño in all these meridional sections (Inoue and Sugimura, 1992). At 160°W and at 180°, the pCO_2(sea) in 1990 reported here showed intermediate values of pCO_2(sea) in these extremes of the ENSO phenomena. On the other hand, pCO_2(sea) at 160°E in 1990 was comparable to that in the mid-El Niño. Wong et al. (1993) reported that the pCO_2(sea), salinity, and nitrate concentrations in the equatorial region between 170°W and 180° decreased while SST increased with the progress of the 1986/87 El Niño. If we compare the data for the same season, pCO_2(sea), salinity, and nitrate concentration between 5°S and 5°N along 180° in September 1990 are smaller than those in August 1986 at the onset of the 1986/87 El Niño and larger than those in September 1987 in the mid-El Niño though SST (29.7°C) is the same as that at the onset of the El Niño (Table 1).

3.3. Longitudinal distributions of pCO_2(sea) in the central and western equatorial Pacific

Longitudinal distributions of pCO_2(sea), SST, and salinity along 5°S are shown in Fig. 6 and the longitudinal distributions of pCO_2(sea), SST, salinity, DIC, and DIN concentration along the equator are shown in Fig. 7. As discussed in the previous section, pCO_2(sea) in the vicinity of the equator was very high at 150°W and 160°W. On the other hand, there observed a steep pCO_2 (sea) gradient between 170°E and 180°. Seawater of the eastern higher pCO_2(sea) region in the central Pacific is characterized by higher salinity (35.1–35.5 psu), lower SST (lower in the east), and higher nutrient concentration (higher in the east)

Table 1. *Averages of oceanographic properties in surface seawater between 5°N and 5°S in the central Pacific*

Longitude	Year	Month	SST (°C)	Salinity (psu)	$[NO_3^-]$ (μmol kg^{-1})	pCO_2(sea) (μatm)	Ref.
170°W–180°	1986	Aug.	29.68	35.274	1.25	403.8	Wong et al. (1993)
170°W–180°	1987	Sep.	30.41	34.500	0.01	346.8	Wong et al. (1993)
180°	1990	Sep.	29.7	34.778	0.30	362.3	present work
179°E	1990	Nov.	29.7	35.055	1.37	388.8	present work

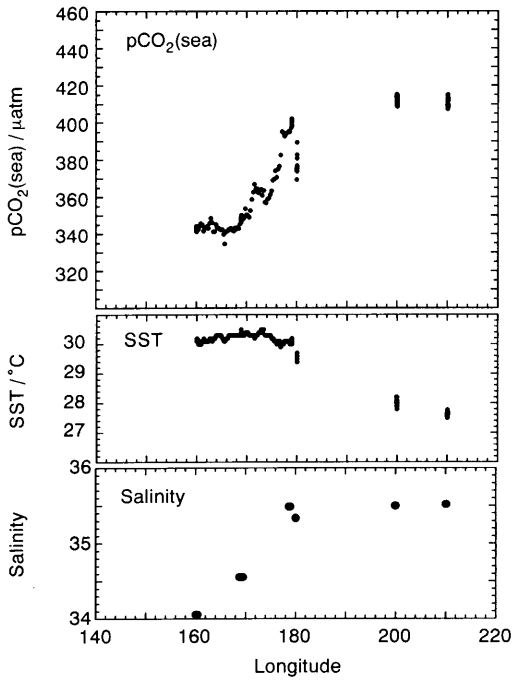

Fig. 6. Longitudinal distributions of pCO_2(sea), SST, and salinity along 5°S.

due to equatorial upwelling, while the western low pCO_2(sea) region is characterized by lower salinity (34.0–34.6 psu), higher SST (above 29.5°C on the equator and above 30°C at 5°S), and depleted nutrients. Less saline surface seawater in the western equatorial Pacific is consistent with the larger freshwater influx as a result of the much precipitation due to strong atmospheric convection over this region (Bryan and Oort, 1984).

Such a steep pCO_2(sea) gradient region was observed near 160°W in January–February 1987 during the 1986/87 El Niño (Inoue and Sugimura, 1988b) and was inferred to locate in the west of 160°E in January–February 1989 during the 1988/89 La Niña (Inoue and Sugimura, 1992). The strong atmospheric convective region over the western equatorial Pacific is known to shift eastward when El Niño condition prevailed (Pazan and Meyers, 1982). The resultant shift of the region with heavy rainfall would be principally responsible for the east-west movements of the steep pCO_2(sea) gradient region associated with ENSO phenomena.

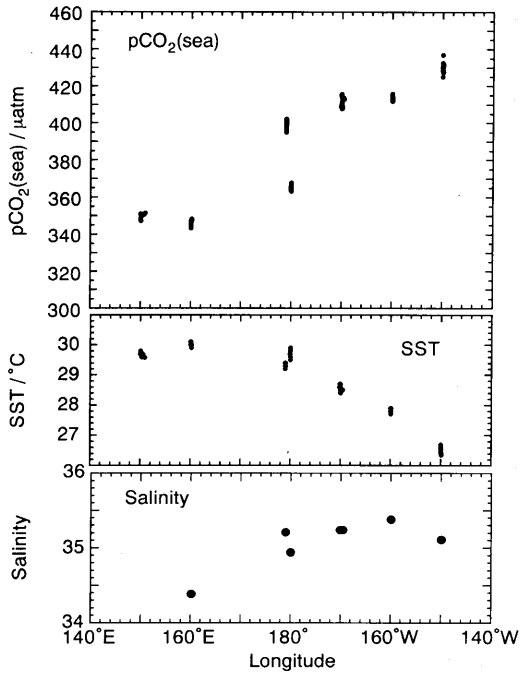

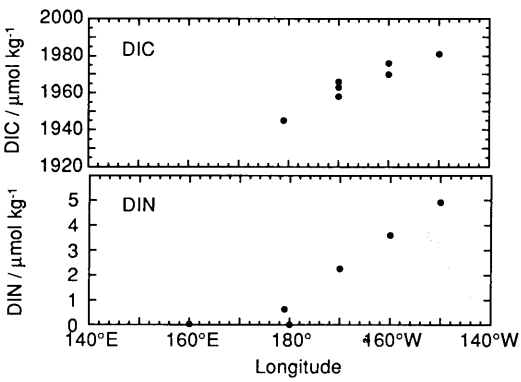

Fig. 7. Longitudinal distributions of pCO_2(sea), SST, salinity, DIC, and DIN along the equator.

The zonal variations of the SST, DIC, and DIN on the equator between 150°W and 179°E where CO_2 in seawater was highly supersaturated were expressed as linear functions of the longitude (Fig. 7). The SST on the equator was elevated from 26.5°C at 150°W to 29.5°C at 179°E which implies 55 μatm increase in pCO_2(sea) through the thermodynamic effect. The pCO_2(sea) has, however, decreased from 430 μatm at 150°W to 400 μatm at 179°E. This pCO_2(sea) decrease is attributable to the DIC decrease of 36 μmol kg^{-1} from

1981 μmol kg^{-1} at 150°W to 1945 μmol kg^{-1} at 179°E. The alkalinity calculated from pCO_2(sea), DIC, SST, and salinity showed an almost uniform zonal distribution with its difference between 150°W and 179°E only 4 μeq kg^{-1}. Therefore, it is inferred that the main reason for the DIC decrease from east to west along the South Equatorial Current (SEC) is the removal of aqueous CO_2 from seawater, possibly by the net biological photosynthetic uptake of CO_2 and the net CO_2 emission through the air-sea interface.

The amount of the net biological CO_2 uptake ($\Delta DIC_{(bio)}$) between 150°W and 179°E was estimated based on the Redfield ratio ($\Delta C:\Delta N:\Delta P = 106:16:1$; Redfield et al., 1963) and the change in DIN concentration. The change in DIN concentration is -4.7 μmol kg^{-1} (5.3 μmol kg^{-1} at 150°W and 0.6 μmol kg^{-1} at 179°E), hence $\Delta DIC_{(bio)}$ is calculated as $-4.7 \cdot 106/16 = -31$ μmol kg^{-1}. It suggests that most of the DIC decrease along the SEC would be attributable to the biological CO_2 uptake. These calculations assume that the upwelled colder water at 150°W is advected steadily toward 179°E while being warmed. It is not likely to be exactly the case, as the SEC in the western Pacific shows a significant variability (Richards and Pollard, 1991) and the meridional and vertical advection and mixing in the equatorial zone of the western meridional sections would not be negligible. Long waves in the eastern equatorial Pacific (Legeckis, 1977) has been reported to influence the distributions of CO_2 species (Feely, et al., 1994) as well as other physical, chemical, and biological properties in the surface waters (Chavez et al., 1990). However, our observations were confined to the west of 150°W, where long waves are not prominent (Legeckis, 1986). The zonal variation of salinity between 150°W and 179°E (except for 180°) along the equator (within 0.27 psu) and along 5°S (within 0.03 psu) are small. Therefore, we think that this assumption would be valid as an approximation for demonstrating the relative importance of the factors which influence the pCO_2(sea) spatial variation.

3.4. *Net CO_2 flux in the central and western equatorial Pacific from September through November 1990*

Air-sea CO_2 flux in the central and western Pacific was estimated for the period between September and November using equations (1) and (3):

$$E = k \cdot S, \tag{3}$$

where k is the gas transfer piston velocity of CO_2 between the sea and the air, and S is the solubility of CO_2 in seawater.

For the flux calculation, the central and western equatorial Pacific (10.5°N–15.5°S and 139.5°E–149.5°W) were divided into 1° by 1° pixels. For the calculation of the CO_2 solubility, we used the empirical formula as functions of SST and salinity given by Weiss (1974). The monthly mean SST in each pixel was calculated by the linear interpolation of the monthly mean SST provided by the Japan Meteorological Agency (JMA) for each 2° by 2° pixel (JMA, 1990a, 1990b, 1990c). The salinity was taken to be 35 psu.

Monthly pCO_2(sea) distributions were evaluated as follows. At first, observed pCO_2(sea) were normalized at 28°C using equation (2) and averaged into one value per degree latitude along the ship track. The averaged normalized pCO_2(sea) were then linearly interpolated to east-west direction except for the longitudinal pCO_2(sea) steep gradient region between 179°E and 160°E where the degree of the normalized pCO_2 decrease from 179°E to 160°E along 5°S were adapted for other latitudes between 5°N and 4°S. The resultant two-dimensional distributions of normalized pCO_2(sea) was transformed into monthly mean pCO_2(sea) distributions using equation (2) and the monthly mean SST distributions described above in order to take the thermodynamic effect of SST monthly variation into account. The observed pCO_2(sea) data in 180° between 5°N and 5°S in September were not used, because they appears to have been influenced by a temporary heavy rainfall as discussed in Subsection 3.2. However, if we assume that such a condition had been prevailing during the most of the period between September and November and use the data along 180° instead of the data along 179°E in November for the evaluation of the two-dimensional pCO_2(sea) distributions, CO_2 outflux from this region estimated become about 8% smaller than that calculated using 179°E data.

The meridional distribution of the atmospheric CO_2 concentration had been observed at least once every month from September through November.

They were averaged into one value per degree latitude along the ship track. The monthly two-dimensional pCO_2(air) distributions were evaluated assuming that pCO_2(air) was constant over the same latitude in the same month. The distribution of ΔpCO_2 was calculated for each month, and that in September 1990 is shown in Fig. 8 as an example.

For the gas transfer piston velocity and the gas transfer coefficient, several equations have been proposed as a function of the wind speed. Liss and Merlivat (1986) and Etcheto and Merlivat (1988) reported the gas transfer piston velocity of CO_2 that depends on the wind speed and the Schmidt number (Sc) (Jahne et al., 1984):

$$k(\text{cm h}^{-1}) = 0.17 U_{10}(\text{Sc}_{20}/\text{Sc})^{2/3},$$
$$0 < U_{10} \leqslant 3.6 \text{ m s}^{-1}, \quad (4a)$$

$$k(\text{cm h}^{-1}) = [2.85 U_{10} - 9.65](\text{Sc}_{20}/\text{Sc})^{1/2},$$
$$3.6 < U_{10} \leqslant 13 \text{ m s}^{-1}, \quad (4b)$$

$$k(\text{cm h}^{-1}) = [5.9 U_{10} - 49.3](\text{Sc}_{20}/\text{Sc})^{1/2},$$
$$U_{10} > 13 \text{ m s}^{-1}, \quad (4c)$$

where U_{10} is the wind speed at 10-m height and Sc_{20} is the Schmidt number at 20°C. We used the Schmidt number in seawater given by Wanninkhof (1992).

Wanninkhof (1992) proposed 3 equations of gas transfer piston velocity. Two of them should be used with the short-term wind speed data and another should be used with the long-term wind speed data. They are quadratic functions of the wind speed.

- short-term:

$$k(\text{cm h}^{-1}) = 0.31 U_{10}^2(\text{Sc}_{20}/\text{Sc})^{1/2}; \quad (5)$$

- short-term with the effect of chemical enhancement taken into account:

$$k(\text{cm h}^{-1}) = [2.5(0.5246 + 1.6256 \times 10^{-2} t + 4.9946 \times 10^{-4} t^2) + 0.31 U_{10}^2] \times (\text{Sc}_{20}/\text{Sc})^{1/2}; \quad (6)$$

- long-term:

$$k(\text{cm h}^{-1}) = 0.39 U_{av}^2(\text{Sc}_{20}/\text{Sc})^{1/2}, \quad (7)$$

where t is SST (°C) and U_{av} is the averaged wind speed (m s^{-1}).

According to Tans et al. (1990), the gas transfer coefficient E is expressed as follows:

$$E(\text{mol m}^{-2} \text{ y}^{-1} \mu\text{atm}^{-1}) = 0.016(U - 3);$$
$$U \geqslant 3 \text{ m s}^{-1} \quad (8)$$

E is taken to be zero for $U \leqslant 3$ m s^{-1}. At present, we can not state which equation would be most reliable, hence we used all five sets of equations (4)–(8) for the CO_2 flux calculation and compared the results.

The other factors which make the current flux estimations ambiguous is incomplete wind speed data and its treatment. We used two data sets of surface wind speed provided by JMA. The GANAL data sets are made on the basis of the radiosonde data for long-term weather forecasting (JMA, 1990e). The meteorological elements such as wind speed, temperature, isobaric height, etc.

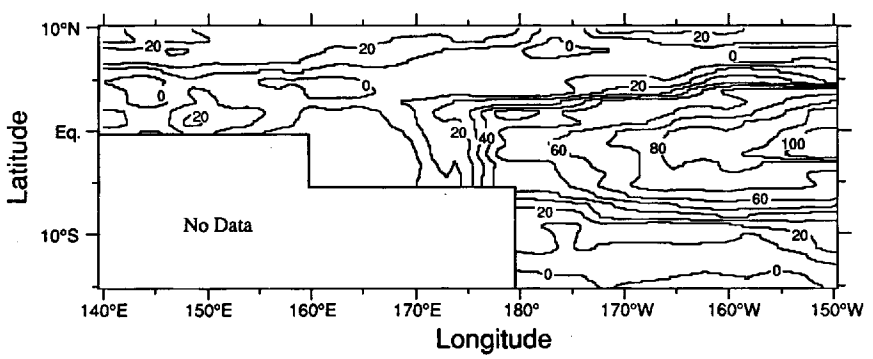

Fig. 8. Distribution of ΔpCO_2 in the central and western equatorial Pacific in September, 1990.

Tellus B/47/4-6

are available twice a day with 1.875° by 1.875° grid points. The monthly mean of wind speed (WSCLI data set) is complied on the basis of observed wind speed on board for the period from 1961 to 1990 (JMA, 1993b). The WSCLI data set covers the North Pacific (0°–69° N, 100° E–70° W) with 1° by 1° pixels. If wind data are missing, we interpolate zonally between contiguous data. The observed monthly mean in 1990 is most appropriate data, but the number of measurements in the equatorial Pacific is too small to calculate CO_2 flux.

Wind speed data observed on board R.V. Hakuho-maru during the cruise (W_{obsd}) were compared with the GANAL surface wind speed data (W_{GANAL}) for the pairs of data at the same time within 10 miles. The linear relationship between W_{obsd} and W_{GANAL} has been calculated by the least squares method. W_{obsd} correlates fairly well with W_{GANAL}:

$$W_{obsd} = 0.728 W_{GANAL} + 2.43 \quad (R = 0.734). \quad (9)$$

The deviations would be mainly attributable to the mesoscale weather which frequently accompanies stronger wind and is not represented in GANAL, and somewhat to the paucity of radiosonde data in the Pacific. The flux calculations along 150° W and 180° showed that the calculated fluxes based on W_{obsd} are approximately 40% larger than those based on W_{GANAL}. In the following calculations, we used wind speed data transformed from the W_{GANAL} data set using the relationship (9). They give approximately 10% smaller fluxes along 150° W and 180° than those based on W_{obsd}.

We calculated CO_2 fluxes by two methods with respect to the wind speed. At first, the flux in each pixel was computed twice a day and accumulated over a month. Secondly, the monthly mean flux in each pixel was computed using monthly averaged wind intensity.

The two-dimensional flux distribution in September 1990 estimated using Liss and Merlivat equations (4a)–(4c) by the accumulation of twice-daily fluxes is shown in Fig. 9 as an example. The larger ΔpCO_2 and generally higher wind speed (6–8 m s^{-1}) in the equatorial region of the central Pacific resulted in a larger CO_2 efflux from this region, and the smaller ΔpCO_2 and generally lower wind speed (3–4 m s^{-1}) resulted in a smaller net flux in the western Pacific.

The results of the flux calculation are summarized in Table 2, where the monthly mean wind speed for 30 years gives somewhat low value as compared with W_{GANAL}. The differences in flux between each month, resulted from SST variation and wind speed variation, are less than 6%. As most wind speeds are in the "rough surface regime" ($3.6 < U_{10} \leqslant 13$ m s^{-1}) where the gas transfer piston velocity given by Liss and Merlivat is a linear function of the wind speed (eq. (4b)), the flux accumulated over a month and the flux calculated based on the monthly averaged wind speed exhibited only small differences if we use their gas transfer piston velocity. This is also the case when the gas transfer coefficient given by Tans et al. (eq. (8)) is used. For the three equations given by Wanninkhof (eqs. (5–7)), the computed fluxes showed only 5% differences between those two methods of calculation. The flux calculated using the short-term equation (eq. (5)) from twice-daily wind speed and that calculated using the long-term equation (eq. (7)) from monthly

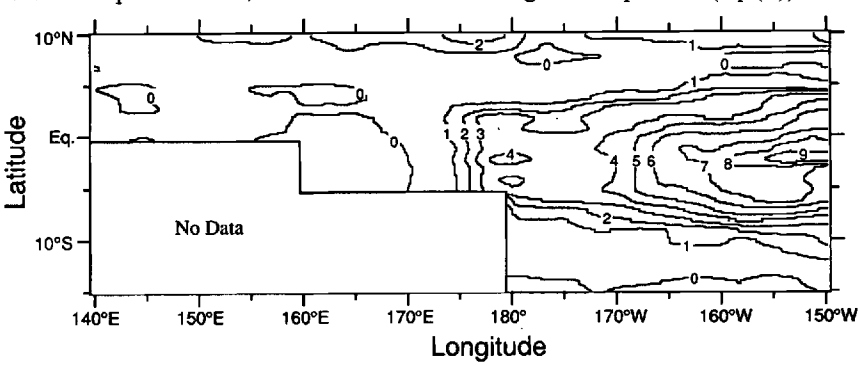

Fig. 9. Distribution of the CO_2 flux (in mmol m^{-2} d^{-1}) in the central and western Pacific in September, 1990. CO_2 flux was computed using the gas transfer piston velocity given by Liss and Merlivat (1986) and twice-daily wind speed data.

Table 2. *CO_2 flux (MtC) in the central and western equatorial Pacific in September–November 1990*

Eq.	Flux (15°S–1°S) (MtC)	Flux (0°–10°N) (MtC)		Total flux (MtC)
(*Flux accumulated twice-daily flux over a month*)	GANAL	GANAL		GANAL
Liss and Merlivat	19.5	13.1		32.6
Wanninkhof (short)	30.2	21.1		51.3
Wanninkhof (short, chem)	36.6	26.8		63.4
Wanninkhof (long)	38.0	26.5		64.5
Tans et al.	42.3	29.0		71.3
(*Flux calculated by using monthly mean wind speed*)	GANAL	GANAL	WSCLI	GANAL
Liss and Merlivat	19.5	12.9	11.4	32.4
Wanninkhof (short)	28.9	19.8	18.5	48.7
Wanninkhof (short, chem)	35.4	25.6	24.4	61.0
Wanninkhof (long)	36.4	24.9	23.3	61.3
Tans et al.	42.2	29.0	25.7	71.2

averaged wind speed exhibited a significant discrepancy. This is because the wind speed distribution can not be approximated to the "Rayleigh probability distribution" in this case for the very limited area and period.

Obviously, the uncertainty in the gas transfer coefficient is the main reason for the ambiguity of the CO_2 flux estimation. As shown in Table 2, net CO_2 flux in the central and western Pacific estimated are between 32.4 MtC and 71.3 MtC per 3 months. A simple extrapolation gives annual values between 0.13 and 0.29 GtC year^{-1}, which have contributions between +0.06 and +0.14 ppm year^{-1} to the atmospheric CO_2 concentration. As our observation was confined to the west of 150°W and the net CO_2 flux from the eastern equatorial Pacific east of 150°W is known to be prominent (Murphy et al., 1991a, 1991b; Lefèvre and Dandonneau, 1992), we can not assess the net CO_2 flux in the whole equatorial Pacific in 1990. However, it seems reasonable to assume that the net CO_2 flux for the central and western Pacific calculated here canbe approximated to a conservative estimate of the flux difference between non-El Niño period and an El Niño period since these regions had only a minor contribution to the net air-sea CO_2 flux during the 1986/88 El Niño event (Inoue and Sugimura, 1992).

The contribution of the CO_2 flux imbalance between the atmosphere and the ocean and/or the terrestrial biosphere to the interannual variation of the atmospheric CO_2 increase associated with ENSO event is still controversial (Siegenthaler, 1990). The decrease of CO_2 release between 0.13 and 0.29 GtC year^{-1} from the central and western equatorial Pacific during an El Niño period implies the equivalent increase of the net CO_2 uptake by the ocean if the steady-state in the global CO_2 air-sea exchange except for the equatorial Pacific is assumed. Keeling et al. (1989) evaluated the anomalous oceanic uptake of 4 GtC in 1982/83 El Niño by a double deconvolution of the interannual variability of the atmospheric CO_2 concentration and that of $\delta^{13}C$ of the atmospheric CO_2. It is more than one order of magnitude larger than our conservative estimate. Volk (1989) and Siegenthaler and Wenk (1989) evaluated the temporary decrease of CO_2 evasion flux from the equatorial Pacific into the atmosphere during an El Niño period using box models as 0.8 GtC year^{-1} and 1.1 GtC year^{-1}, respectively. Winguth et al. (1994) predicted a temporary CO_2 uptake of 0.6 GtC by the ocean in 1983 during the 1982/83 El Niño using a three dimensional ocean circulation model coupled with an oceanic carbon cycle model. These three model estimates are rather comparable to our estimate based on the direct pCO_2 observations.

4. Conclusion

Measurements of CO_2 in and over the central and western Pacific west of 150°W were made

during the period from September to December 1990. The data presented in this paper are available on floppy disks from the authors and will be available from the Japan Climatic Data Center, Japan Meteorological Agency.

The equatorial Pacific can be divided into two areas with respect to pCO_2(sea): In the eastern high pCO_2(sea) region east of 179° E with lower SST, higher salinity and not-depleted nutrients, pCO_2(sea) showed a maximum value over 440 μatm at 150° W, which is attributed to strong equatorial upwelling. The pCO_2(sea) decreased to the west which can be explained by a combination of the effects of biological CO_2 uptake, the probably less important DIC decrease due to air-sea CO_2 exchange, and SST rise during the zonal flow toward the west. The concentration of nutrients became almost 0 μmol kg^{-1} at 180°. In the western region where SST was higher, salinity was lower, and nutrients were depleted, pCO_2(sea) was nearly the same level as pCO_2(air). The steep change of pCO_2(sea) in the equatorial Pacific between 170° E and 179° E was accompanied by a salinity change, i.e., the effect of rainfall on pCO_2(sea). This steep gradient region moves east-west associated with ENSO phenomena.

In the subtropical region south of 12° S at 150° W and south of 10° S at 180°, the meridional variation of pCO_2(sea) was attributable to SST variations through the thermodynamic effect. On the NECC flowing eastward between 5° N and 10° N, the pCO_2(sea) was nearly the same level as pCO_2(air).

The net CO_2 flux from the sea to the atmosphere in the equatorial zone of the central and western Pacific was estimated as 0.13 to 0.29 GtC year^{-1}. The ambiguity arises mainly from the uncertainty of the gas transfer coefficients used. This flux gives a conservative estimate of the flux difference in the central and western equatorial Pacific between a non-El Niño period and a El Niño period, and it is comparable to the estimates by the model simulations of the equatorial Pacific during an El Niño event.

5. Acknowledgments

We thank Dr. M. Terazaki, chief scientist of the KH-90-2 cruise, Dr. H. Sakai and Dr. Y. Nozaki, chief scientists of the KH-90-3 cruise, and the officers and crew of the R.V. Hakuho-maru belonging to Ocean Research Institute, the University of Tokyo. We also wish to thank Dr. Saino for his helpful suggestions, providing the data for several oceanic properties and ADCP data, and Mr. H. Otobe and Mr. H. Hasumoto for providing the meteorological data during the cruises. We should like to thank anonymous reviewers for their helpful discussion.

REFERENCES

Berger, W. H. 1989. Global maps of ocean productivity. In: *Productivity of the ocean: present and past* (eds. W. H. Berger, V. S. Smetacek and G. Wefer). John Wiley & Sons, Chichester, 429–455.

Broecker, W., Peng, T.-H., Ostlund, G. and Stuiver, M. 1985. The distribution of bomb radiocarbon in the ocean. *J. Geophys. Res.* **90**, 6953–6970.

Bryan, F. and Oort, A. 1984. Seasonal variation of the global water balance based on aerological data. *J. Geophys. Res.* **89**, 11717–11730.

Chavez, F. P., Buck, K. R. and Barber, R. T. 1990. Phytoplankton taxa in relation to primary production in the equatorial Pacific. *Deep-Sea Res.* **37**, 1733–1752.

Dickson, A. G. and Millero, F. J. 1987. A comparison of the equilibrium constants for the dissociation of carbonic acid in seawater media. *Deep-Sea Res.* **34**, 1733–1743.

Etcheto, J. and Merlivat, L. 1988. Satellite determination of the carbon dioxide exchange coefficient at the ocean-atmosphere interface: A first step. *J. Geophys. Res.* **93**, 15669–15678.

Feely, R. A., Gammon, R. H., Taft, B. A., Pullen, P. E., Waterman, L. S., Conway, T. J., Gendron, J. F. and Wisegarver, D. P. 1987. Distribution of chemical tracers in the eastern equatorial Pacific during and after the 1982–83 El Niño/Southern Oscillation Event. *J. Geophys. Res.* **92**, 6545–6558.

Feely, R. A., Wanninkhof, C. E., Cosca, C. E., McPhaden, M. J., Byrne, R. H., Millero, F. J., Chavez, F. P., Clayton, T., Campbell, D. M. and Murphy, P. P. 1994. The effect of tropical instability waves on CO_2 species distributions along the equator in the eastern equatorial Pacific during the 1992 ENSO event. *Geophys. Res. Letters* **21**, 277–280.

Fushimi, K. 1987. Variation of carbon dioxide partial pressure in the western North Pacific surface water during the 1982/83 El Niño event. *Tellus* **39B**, 214–227.

Gordon, L. I. and Jones, L. B. 1973. The effect of temperature on carbon dioxide partial pressure in sea water. *Mar. Chem.* **1**, 317–322.

Inoue, H., Sugimura, Y. and Fushimi, K. 1987. pCO_2 and $\delta^{13}C$ in the air and surface sea water in the western North Pacific. *Tellus* **39B**, 228–242.

Inoue, H. and Sugimura, Y. 1988a. Distribution and variations of oceanic carbon dioxide in the western North Pacific, eastern Indian, and Southern Ocean south of Australia. *Tellus* **40B**, 308–320.

Inoue, H. and Sugimura, Y. 1988b. Distribution of the pCO_2 in surface seawater of the western and central equatorial Pacific during the 1986/87 El Niño/Southern Oscillation event. *Geophys. Res. Letters* **15**, 1499–1502.

Inoue, H. and Sugimura, Y. 1992. Variations and distributions of CO_2 in and over the equatorial Pacific during the period from the 1986/88 El Niño event to the 1988/89 La Niña event. *Tellus* **44B**, 1–22.

IPCC. 1990. *The IPCC scientific assessment* (eds. J. T. Houghton, G. J. Jenkins, and J. J. Ephraums). Cambridge Univ. Press.

Jahne, B., Huber, W., Dutzi, A., Wais, T. and Ilmberger, J. 1984. Wind/wave tunnel experiment on the Schmidt number and wind field dependence of air/water exchange. In: *Gas transfer at water surfaces* (eds. W. Brutsaert and G. H. Jirka). Dordrecht/Holland: D. Reidel Publ. Comp., 237–246.

JMA 1990a, 1990b, 1990c, 1990d. *Monthly report on climate system* 90-09, 90-10, 90-11, 90-12, Japan Meteorological Agency, Tokyo.

JMA 1990e. 15-L Global analysis monthly tape data set. In: *Monthly tape for GL-objective analysis data set on Lat-Lon grid and GL-spectral model with complete physics.* Japan Meteorological Agency, Tokyo.

JMA 1991. *Report of observations for monitoring background marine pollution* **38**, *Results in 1990.* Japan Meteorological Agency, Tokyo.

JMA 1992. *Report of observations for monitoring background marine pollution* **39**, *Results in 1991.* Japan Meteorological Agency, Tokyo.

JMA 1993a. *Monthly Ocean Report* 1. El Niño Monitoring Center, Japan Meteorological Agency, Tokyo.

JMA 1993b. *Marine climatological charts of the North Pacific Ocean for a 30-year period.* Japan Meteorological Agency, Tokyo.

Keeling, C. D. 1958. The concentration and isotopic abundance of carbon dioxide in rural areas. *Geochim. Cosmochim. Acta* **13**, 322–334.

Keeling, C. D. 1961. The concentration and isotopic abundance of carbon dioxide in rural and marine air. *Geochim. Cosmochim. Acta* **24**, 277–334.

Keeling, C. D. and Revelle, R. 1985. Effects of El Niño/Southern Oscillation on the atmospheric content of carbon dioxide. *Meteoritics* **20**, 437–450.

Keeling, C. D., Bacastow, R. B., Carter, A. F., Piper, S. C., Whorf, T. P., Heimann, M., Mook, W. G. and Roeloffzen, H. 1989. A three-dimensional model of atmospheric CO_2 transport based on observed winds (1). Analysis of observational data. In: Aspects of climate variability in the Pacific and the western Americas. *Geophysical Monograph* **55** (ed. D. H. Peterson). Am. Geophys. Un., Washington DC, 165–236.

Lefevre, N. and Dandonneau, Y. 1992. Air-sea CO_2 fluxes in the equatorial Pacific in January–March 1991. *Geophys. Res. Letters* **19**, 2223–2226.

Legeckis, R. 1977. Long waves in the eastern equatorial Pacific Ocean: a view from a geostationary satellite. *Science* **197**, 1179–1181.

Legeckis, R. 1986. Long waves in the equatorial Pacific and Atlantic Oceans during 1983. *Ocean-Air Interactions* **1**, 1–101.

Levitus, S. 1982. Climatological atlas of the world ocean. *NOAA professional paper* **13**, 174.

Liss, P. and Merlivat, L. 1986. Air-sea gas exchange rates: Introduction and synthesis. In: *The role of air-sea exchange in geochemical cycling* (ed. P. Buat-Menard). Dordrecht/Holland: D. Reidel Publ. Comp. 113–127.

Matsueda, H., Inoue, H. and Ishii, M. 1993. Latitudinal distributions of methane in the upper troposphere and marine boundary air over the Pacific in 1990. *Geophys. Res. Letters* **20**, 695–698.

Murphy, P. P., Feely, R. A., Gammon, R. H., Kelly, K. C. and Waterman, L. S. 1991a. Autumn air-sea disequilibrium of CO_2 in the South Pacific Ocean. *Mar. Chem.* **35**, 77–84.

Murphy, P. P., Feely, R. A., Gammon, R. H., Harrison, D. E., Kelly, K. C. and Waterman, L. S. 1991b. Assessment of the air-sea exchange of CO_2 in the South Pacific during austral autumn. *J. Geophys. Res.* **96**, 20455–20465.

Nydal, R. and Lövseth, K. 1983. Tracing bomb ^{14}C in the atmosphere 1962–1980. *J. Geophys. Res.* **88**, 3621–3642.

Okazaki, M. 1993. Calcium carbonate formation by calcareous algae. Its mechanisms and productivity in ocean. *Chikyukagaku* (*Geochemistry*) **27**, 29–36.

Pazan, S. and Meyers, G. 1982. Pacific trade wind fluctuations and the Southern Oscillation Index. *Mon. Weather Rev.* **110**, 587–600.

Philander, S. G. 1990. *El Niño, La Niña, and the Southern Oscillation.* Academic Press, San Diego.

Redfield, A. C., Ketchum, B. H. and Richards, F. A. 1963. The influence of organisms on the composition of seawater. In: *The sea* **2** (ed. M. N. Hill). Wiley-Interscience, New York, 26–27.

Richards, K. J. and Pollard, R. T. 1991. Structure of the upper ocean in the western equatorial Pacific. *Nature* **350**, 48–50.

Siegenthaler, U. 1986. Carbon dioxide: its natural cycle and anthropogenic perturbation. In: *The role of air-sea exchange in geochemical cycling* (ed. P. Buat-Menard). Dordrecht/Holland: D. Reidel Publ. Comp. pp. 209–247.

Siegenthaler, U. 1990. El Niño and atmospheric CO_2. *Nature* **345**, 295–296.

Siegenthaler, U. and Sarmiento, J. L. 1993. Atmospheric carbon dioxide and the ocean. *Nature* **365**, 119–125.

Siegenthaler, U. and Wenk, T. 1989. Modeling the Ocean's role for El Niño-related CO_2 variations. In: *Extended Abstr. 3rd International Conference on analysis and evaluation of atmospheric CO_2 data present and past. Environmental Pollution Monitoring and Research Programme* **59**. World Meteorological Organization, Geneva, 189–194.

Tanaka, M., Nakazawa, T. and Aoki, S. 1987. Time and Space variations of tropospheric carbon dioxide over Japan. *Tellus* **39B**, 3–12.

Tans, P. P., Fung, I. Y. and Takahashi, T. 1990. Observational constraints on the global atmospheric CO_2 budget. *Science* **247**, 1431–1438.

Volk, T. 1989. Effect of equatorial Pacific upwelling on atmospheric CO_2 during the 1982–83 El Niño. *Global Biogeochem. Cycles* **3**, 267–279.

Wagner, K. 1979. The carbonate system of the ocean. In: *The global carbon cycle. Scientific Committee on Problems of the Environment of the International Council of Scientific Unions* **13** (eds. B. Bolin, E. T. Degens, S. Kempe and P. Ketner). John Wiley & Sons, Chichester, 251–258.

Wanninkhof, R. 1992. Relationship between wind speed and gas exchange over the ocean. *J. Geophys. Res.* **97**, 7373–7382.

Weiss, R. F. 1974. Carbon dioxide in water and seawater: the solubility of a non-ideal gas. *Mar. Chem.* **2**, 203–215.

Weiss, R. F., Jahnke, R. A. and Keeling, C. D. 1982. Seasonal effects of temperature and salinity on the partial pressure of CO_2 in seawater. *Nature* **300**, 511–513.

Winguth, A. M. E., Heimann, M., Kurtz, K. D., Maier-Reimer, E., Mikolajewicz, U. and Segschneider, J. 1994. El Niño-Southern Oscillation related fluctuations of the marine carbon cycle. *Global Biogeochem. Cycles* **8**, 39–63.

WMO, 1992. WMO WDCGG Data Report, Part A (Carbon Dioxide), GAW Data, Vol. IV. *Greenhouse gases and other atmospheric gases*, WDCGG **2**, The Japan Meteorological Agency in cooperation with the World Meteorological Organization, Tokyo.

Wong, C. S., Chan, Y.-H., Page, J. S., Smith, G. E. and Bellegay, R. D. 1993. Changes in equatorial CO_2 flux and new production estimated from CO_2 and nutrient levels in Pacific surface waters during the 1986/87 El Niño. *Tellus* **45B**, 64–79.